The Optimized Effective Potential Method of Density Functional Theory: Applications to Atomic and Molecular Systems

T. Grabo and E.K.U. Gross

Institut für Theoretische Physik, Universität Würzburg, Am Hubland, D-97074 Würzburg, Germany

Abstract

Using the optimized effective potential method in conjunction with the semi-analytical approximation due to Krieger, Li and Iafrate, we have performed fully self-consistent exact exchange-only density-functional calculations for diatomic molecules with a fully numerical basis-set-free molecular code. The results are very similar to the ones obtained with the Hartree Fock approach. Furthermore we present results for ground states of positive atomic ions including correlation contributions in the approximation of Colle and Salvetti. It is found that the scheme performs significantly better than conventional Kohn-Sham calculations.

1   Introduction

Since its development by Talman and Shadwick [1], following the original idea of Sharp and Horton [2], the optimized effective potential (OEP) method has been recognized [3, 4] as the exact implementation of exchange-only density functional theory (DFT) [5, 6, 7, 8]. Due to the rather large computational effort involved, this scheme has not been used extensively. In the last years, however, the situation has changed. Using an accurate analytical approximation due to Krieger, Li and Iafrate (KLI) [9, 10, 11] the effort involved in numerical calculations based on the OEP has become comparable to conventional Kohn-Sham calculations, while the gain in accuracy is considerable.

In the following, we will briefly review the theoretical foundations of the OEP method and the KLI approximation and present, in section 3, applications of the

method to molecular systems. Finally, in section 4, calculations for atomic systems including correlation effects are discussed and compared with conventional Kohn-Sham results.

2   Basic formalism

We start from ordinary spin DFT [12, 13], where the basic variables are the spin-up and spin-down densities $\rho_\uparrow(\mathbf{r})$ and $\rho_\downarrow(\mathbf{r})$, respectively. They are obtained by self-consistently solving the single-particle Schrödinger equations (atomic units are used throughout)

$$\left(-\frac{\nabla^2}{2} + V_\sigma[\rho_\uparrow, \rho_\downarrow](\mathbf{r})\right) \varphi_{j\sigma}(\mathbf{r}) = \varepsilon_{j\sigma}\varphi_{j\sigma}(\mathbf{r}) \qquad j = 1, \ldots, N_\sigma \qquad \sigma = \uparrow, \downarrow \quad (1)$$

where

$$\rho_\sigma(\mathbf{r}) = \sum_{i=1}^{N_\sigma} |\varphi_{i\sigma}(\mathbf{r})|^2, \tag{2}$$

The Kohn-Sham potentials $V_\sigma(\mathbf{r})$ may be written in the usual way as

$$V_\sigma(\mathbf{r}) = v_{\text{ext}}(\mathbf{r}) + \int d^3r' \, \frac{\rho(\mathbf{r}')}{|\mathbf{r} - \mathbf{r}'|} + V_{\text{xc}\sigma}(\mathbf{r}), \tag{3}$$

$$\rho(\mathbf{r}) = \sum_{\sigma = \uparrow, \downarrow} \rho_\sigma(\mathbf{r}) \tag{4}$$

where $v_{\text{ext}}(\mathbf{r})$ represents the Coulomb potential of the nuclei and $V_{\text{xc}\sigma}(\mathbf{r})$ is a *local* exchange-correlation (xc) potential formally defined as functional derivative of the xc energy

$$V_{\text{xc}\sigma}(\mathbf{r}) := \frac{\delta E_{\text{xc}}[\rho_\uparrow, \rho_\downarrow]}{\delta \rho_\sigma(\mathbf{r})}. \tag{5}$$

In order to understand the nature of the OEP method we recall that the Hohenberg-Kohn theorem [5], applied to non-interacting systems, ensures that the ground-state determinant and hence all occupied orbitals are unique functionals of the spin densities:

$$\varphi_{j\sigma}(\mathbf{r}) = \varphi_{j\sigma}[\rho_\uparrow, \rho_\downarrow](\mathbf{r}). \tag{6}$$

As a consequence of (6), *any orbital functional $E_{\text{xc}}[\{\varphi_{j\tau}\}]$ is an implicit functional of $\rho_\uparrow$ and $\rho_\downarrow$*, provided that the orbitals come from a *local* potential.

The starting point of the so-called OEP method is the total energy functional

$$\begin{aligned} E_{\text{tot}}^{\text{OEP}}[\rho_\uparrow, \rho_\downarrow] &= \sum_{\sigma = \uparrow, \downarrow} \sum_{i=1}^{N_\sigma} \int d^3r \, \varphi_{i\sigma}^*(\mathbf{r}) \left(-\frac{1}{2}\nabla^2\right) \varphi_{i\sigma}(\mathbf{r}) \\ &+ \int d^3r \, v_{\text{ext}}(\mathbf{r})\rho(\mathbf{r}) \\ &+ \frac{1}{2} \int d^3r \int d^3r' \, \frac{\rho(\mathbf{r})\rho(\mathbf{r}')}{|\mathbf{r} - \mathbf{r}'|} \\ &+ E_{\text{xc}}^{\text{OEP}}[\{\varphi_{j\tau}\}] \end{aligned} \tag{7}$$

2

where, in contrast to ordinary spin DFT, the xc energy is an *explicit* (approximate) functional of spin orbitals and therefore only an *implicit* functional of the spin densities $\rho_\uparrow$ and $\rho_\downarrow$. As a consequence of this fact, the calculation of the xc potentials from Eq. (5) is somewhat more complicated: We use the chain rule for functional derivatives to obtain

$$
\begin{aligned}
V_{\mathrm{xc}\sigma}^{\mathrm{OEP}}(\mathbf{r}) &= \frac{\delta E_{\mathrm{xc}}^{\mathrm{OEP}}\left[\{\varphi_{j\tau}\}\right]}{\delta\rho_\sigma(\mathbf{r})} \\
&= \sum_{\alpha=\uparrow,\downarrow}\sum_{i=1}^{N_\alpha}\int d^3 r'\, \frac{\delta E_{\mathrm{xc}}^{\mathrm{OEP}}\left[\{\varphi_{j\tau}\}\right]}{\delta\varphi_{i\alpha}(\mathbf{r}')}\frac{\delta\varphi_{i\alpha}(\mathbf{r}')}{\delta\rho_\sigma(\mathbf{r})} + c.c. \quad (8)
\end{aligned}
$$

and, by applying the functional chain rule once more,

$$
V_{\mathrm{xc}\sigma}^{\mathrm{OEP}}(\mathbf{r}) = \sum_{\alpha=\uparrow,\downarrow}\sum_{\beta=\uparrow,\downarrow}\sum_{i=1}^{N_\alpha}\int d^3 r'\int d^3 r''\left(\frac{\delta E_{\mathrm{xc}}^{\mathrm{OEP}}\left[\{\varphi_{j\tau}\}\right]}{\delta\varphi_{i\alpha}(\mathbf{r}')}\frac{\delta\varphi_{i\alpha}(\mathbf{r}')}{\delta V_\beta(\mathbf{r}'')} + c.c.\right)\frac{\delta V_\beta(\mathbf{r}'')}{\delta\rho_\sigma(\mathbf{r})}.
$$
$$(9)$$

The last term on the right-hand side is readily identified with the inverse $\chi_{\mathrm{s}}^{-1}(\mathbf{r},\mathbf{r}')$ of the density response function of a system of non-interacting particles

$$
\chi_{\mathrm{s}\alpha,\beta}\left(\mathbf{r},\mathbf{r}'\right) := \frac{\delta\rho_\alpha(\mathbf{r})}{\delta V_\beta(\mathbf{r}')}. \quad (10)
$$

This quantity is diagonal with respect to the spin variables so that Eq. (9) reduces to

$$
V_{\mathrm{xc}\sigma}^{\mathrm{OEP}}(\mathbf{r}) = \sum_{\alpha=\uparrow,\downarrow}\sum_{i=1}^{N_\alpha}\int d^3 r'\int d^3 r''\left(\frac{\delta E_{\mathrm{xc}}^{\mathrm{OEP}}\left[\{\varphi_{j\tau}\}\right]}{\delta\varphi_{i\alpha}(\mathbf{r}')}\frac{\delta\varphi_{i\alpha}(\mathbf{r}')}{\delta V_\sigma(\mathbf{r}'')} + c.c.\right)\chi_{\mathrm{s}\sigma}^{-1}\left(\mathbf{r}'',\mathbf{r}\right).
$$
$$(11)$$

Acting with the response operator (10) on both sides of Eq. (11) one obtains

$$
\int d^3 r'\, V_{\mathrm{xc}\sigma}^{\mathrm{OEP}}(\mathbf{r}')\chi_{\mathrm{s}\sigma}\left(\mathbf{r}',\mathbf{r}\right) = \sum_{\alpha=\uparrow,\downarrow}\sum_{i=1}^{N_\alpha}\int d^3 r'\, \frac{\delta E_{\mathrm{xc}}^{\mathrm{OEP}}\left[\{\varphi_{j\tau}\}\right]}{\delta\varphi_{i\alpha}(\mathbf{r}')}\frac{\delta\varphi_{i\alpha}(\mathbf{r}')}{\delta V_\sigma(\mathbf{r})} + c.c..
$$
$$(12)$$

Finally, the second functional derivative on the right-hand side of Eq. (12) is calculated using first-order perturbation theory. This yields

$$
\frac{\delta\varphi_{i\alpha}(\mathbf{r}')}{\delta V_\sigma(\mathbf{r})} = \delta_{\alpha,\sigma}\sum_{\substack{k=1\\k\neq i}}^{\infty}\frac{\varphi_{k\sigma}(\mathbf{r}')\varphi_{k\sigma}^*(\mathbf{r})}{\varepsilon_{i\sigma}-\varepsilon_{k\sigma}}\varphi_{i\sigma}(\mathbf{r}). \quad (13)
$$

Using the fact that the Kohn-Sham response function can be written as

$$
\chi_{\mathrm{s}\sigma}\left(\mathbf{r},\mathbf{r}'\right) = \sum_{i=1}^{N_\sigma}\sum_{\substack{k=1\\k\neq i}}^{\infty}\frac{\varphi_{i\sigma}^*(\mathbf{r})\varphi_{k\sigma}(\mathbf{r})\varphi_{k\sigma}^*(\mathbf{r}')\varphi_{i\sigma}(\mathbf{r}')}{\varepsilon_{i\sigma}-\varepsilon_{k\sigma}} + c.c. \quad (14)
$$

the integral equation (12) takes the form

$$
\sum_{i=1}^{N_\sigma}\int d^3 r'\left(V_{\mathrm{xc}\sigma}^{\mathrm{OEP}}(\mathbf{r}') - u_{\mathrm{xc}i\sigma}(\mathbf{r}')\right)G_{\mathrm{s}i\sigma}\left(\mathbf{r}',\mathbf{r}\right)\varphi_{i\sigma}(\mathbf{r})\varphi_{i\sigma}^*(\mathbf{r}') + c.c. = 0 \quad (15)
$$

3

where

$$u_{\mathrm{xc}i\sigma}(\mathbf{r}) := \frac{1}{\varphi_{i\sigma}^*(\mathbf{r})} \frac{\delta E_{\mathrm{xc}}^{\mathrm{OEP}}[\{\varphi_{j\tau}\}]}{\delta \varphi_{i\sigma}(\mathbf{r})} \tag{16}$$

and

$$G_{\mathrm{s}i\sigma}(\mathbf{r}, \mathbf{r}') := \sum_{\substack{k=1 \\ k \neq i}}^{\infty} \frac{\varphi_{k\sigma}(\mathbf{r})\varphi_{k\sigma}^*(\mathbf{r}')}{\varepsilon_{i\sigma} - \varepsilon_{k\sigma}}. \tag{17}$$

The derivation of the OEP integral equation (15) described here was first given by Görling and Levy [14]. It is important to note that the same expression results [1, 9, 15] if one demands that the local one-particle potential appearing in Eq. (1) be the *optimized* one yielding orbitals minimizing the total energy functional (7), i.e. that

$$\left. \frac{\delta E_{tot}^{OEP}}{\delta V_\sigma(\mathbf{r})} \right|_{V=V^{OEP}} = 0. \tag{18}$$

The main advantage of the OEP method is that it allows for the *exact* treatment of the exchange energy. Splitting up the total xc-functional into an exchange and a correlation part

$$E_{\mathrm{xc}}^{\mathrm{OEP}}[\{\varphi_{j\tau}\}] = E_{\mathrm{x}}[\{\varphi_{j\tau}\}] + E_{\mathrm{c}}[\{\varphi_{j\tau}\}] \tag{19}$$

we can use the exact Fock expression

$$E_{\mathrm{x}}[\{\varphi_{j\tau}\}] = -\frac{1}{2} \sum_{\sigma=\uparrow,\downarrow} \sum_{i,k=1}^{N_\sigma} \int d^3r \int d^3r' \, \frac{\varphi_{i\sigma}^*(\mathbf{r})\varphi_{k\sigma}^*(\mathbf{r}')\varphi_{k\sigma}(\mathbf{r})\varphi_{i\sigma}(\mathbf{r}')}{|\mathbf{r} - \mathbf{r}'|}. \tag{20}$$

Performing the functional derivative with respect to the orbitals one obtaines for the x-part $u_{\mathrm{x}i\sigma}(\mathbf{r})$ of the function $u_{\mathrm{xc}i\sigma}(\mathbf{r})$:

$$u_{\mathrm{x}i\sigma}(\mathbf{r}) = -\frac{1}{\varphi_{i\sigma}^*(\mathbf{r})} \sum_{k=1}^{N_\sigma} \varphi_{k\sigma}^*(\mathbf{r}) \int d^3r' \, \frac{\varphi_{i\sigma}^*(\mathbf{r}')\varphi_{k\sigma}(\mathbf{r}')}{|\mathbf{r} - \mathbf{r}'|}. \tag{21}$$

The use of the exact exchange energy has several advantages over the conventional *explicitly* density dependent xc functionals. Most importantly it ensures the correct $-1/r$ decay of the xc-potential for large r, reflecting the fact that it is self-interaction free. One has to emphasize that the OEP has the correct $-1/r$ tail for *all* orbitals, i.e. for both the occupied and the unoccupied ones. By contrast, the conventional Hartree-Fock (HF) approach, which uses the same expression (20) for the exchange energy but a *nonlocal* potential defined via the equation

$$\left(\hat{V}_{\mathrm{x}\sigma}^{\mathrm{HF}}\varphi_{i\sigma}\right)(\mathbf{r}) = -\sum_{j=1}^{N_\sigma} \int d^3r' \frac{\varphi_{j\sigma}^*(\mathbf{r}')\varphi_{i\sigma}(\mathbf{r}')}{|\mathbf{r} - \mathbf{r}'|}\varphi_{j\sigma}(\mathbf{r}) \tag{22}$$

is self-interaction free only for the *occupied* orbitals. However, x-only OEP calculations [1, 16, 17, 18, 19, 9], i.e. with the approximation $E_{\mathrm{c}}[\{\varphi_{j\tau}\}] = 0$, performed on atomic systems have shown that the results for various *physical* quantities of interest such as total ground-state energies are very similar to HF results despite the different nature of the corresponding x-potentials. As - by construction - the

4

HF scheme gives the variationally best, i.e. lowest, total energy, the x-only OEP solutions are always slightly higher in energy.

The solution of the full integral equation (15) is numerically very demanding and has been achieved so far only for systems with spherical symmetry [1, 16, 17, 18, 19, 9]. Therefore, one has to resort to further approximations for practical reasons. Krieger, Li and Iafrate [9] have suggested the analytical approximation

$$G_{si\sigma}\left(\mathbf{r}, \mathbf{r}'\right) \approx \frac{1}{\triangle\epsilon}\left(\delta\left(\mathbf{r} - \mathbf{r}'\right) - \varphi_{i\sigma}(\mathbf{r})\varphi_{i\sigma}^*(\mathbf{r}')\right) \tag{23}$$

for the Green's-function-type quantity (17). Substituting this into the integral equation (15) and performing some algebra one arrives at the approximate equation

$$V_{\text{xc}\sigma}^{\text{KLI}}(\mathbf{r}) = \frac{1}{2\rho_\sigma(\mathbf{r})}\sum_{i=1}^{N_\sigma}|\varphi_{i\sigma}(\mathbf{r})|^2\left[u_{\text{xc}i\sigma}(\mathbf{r}) + \left(\bar{V}_{\text{xc}i\sigma}^{\text{KLI}} - \bar{u}_{\text{xc}i\sigma}\right) + c.c.\right] \tag{24}$$

where $\bar{u}_{\text{xc}j\sigma}$ denotes the average value of $u_{\text{xc}j\sigma}(\mathbf{r})$ taken over the density of the $j\sigma$ orbital, i.e.

$$\bar{u}_{\text{xc}j\sigma} = \int d^3r \, |\varphi_{j\sigma}(\mathbf{r})|^2 u_{\text{xc}j\sigma}(\mathbf{r}) \tag{25}$$

and similarly for $\bar{V}_{\text{xc}\sigma}^{\text{KLI}}$. In contrast to the exact integral equation (15) the KLI equation (24) can be solved explicitly for $V_{\text{xc}\sigma}$ by multiplication with $\rho_{i\sigma}(\mathbf{r})$ and subsequent integration. This leads to linear $(N_\sigma - 1) \times (N_\sigma - 1)$ equations for the unknown constants $\left(\bar{V}_{\text{xc}i\sigma} - \bar{u}_{\text{xc}i\sigma}\right)$:

$$\sum_{i=1}^{N_\sigma-1}\left(\delta_{ji} - M_{ji\sigma}\right)\left(\bar{V}_{\text{xc}i\sigma}^{\text{KLI}} - \frac{1}{2}\left(\bar{u}_{\text{xc}i\sigma} + \bar{u}_{\text{xc}i\sigma}^*\right)\right) = \bar{V}_{\text{xc}j\sigma}^S - \frac{1}{2}\left(\bar{u}_{\text{xc}j\sigma} + \bar{u}_{\text{xc}j\sigma}^*\right) \tag{26}$$

with $j = 1, \ldots, N_\sigma - 1$,

$$M_{ji\sigma} := \int d^3r \, \frac{|\varphi_{j\sigma}(\mathbf{r})|^2|\varphi_{i\sigma}(\mathbf{r})|^2}{\rho_\sigma(\mathbf{r})} \tag{27}$$

and

$$\bar{V}_{\text{xc}j\sigma}^S(\mathbf{r}) := \int d^3r \, \frac{|\varphi_{j\sigma}(\mathbf{r})|^2}{\rho_\sigma(\mathbf{r})}\sum_{i=1}^{N_\sigma}|\varphi_{i\sigma}(\mathbf{r})|^2\frac{1}{2}\left(u_{\text{xc}i\sigma}(\mathbf{r}) + u_{\text{xc}i\sigma}^*(\mathbf{r})\right). \tag{28}$$

The orbitals corresponding to the highest single-particle energy eigenvalues ε_{N_σ} have to be excluded from the linear equations (26) in order to ensure the correct long-range behaviour of $V_{\text{xc}\sigma}^{\text{OEP}}(\mathbf{r})$ [9]. It is an important property of the KLI approximation that it is exact for two-particle systems, where one has only one electron per spin projection. In this case, the OEP integral equation (15) may be solved exactly to yield (24). Furthermore, for these systems the OEP is also identical with the HF potential (22).

At first sight, the KLI approximation (23) might appear rather crude. The final result (24) for the KLI potential, however, can also be understood [20] as a well-defined mean-field approximation. Explicit calculations on atoms performed in the x-only limit [9, 10, 11] show that the KLI-approximation yields excellent results which differ only by a few ppm from the much more time-consuming exact solutions of the full integral equation (15).

3 Exchange-only results for molecular systems

In order to demonstrate the validity of the KLI-approach for more complex systems, we have performed x-only OEP calculations for diatomic molecules in KLI approximation employing the exact exchange energy functional as defined by equation (20) and neglecting correlation effects. This approach will, in the following, be referred to as *x-only KLI*. Our calculations have been performed with a fully numerical basis-set-free code, developed from the Xα program written by Laaksonen, Sundholm and Pyykkö [21, 22, 23]. The code solves the one-particle Schrödinger equation for diatomic molecules

$$
\left(-\frac{\nabla^2}{2} - \frac{Z_1}{|\mathbf{R}_1 - \mathbf{r}|} - \frac{Z_2}{|\mathbf{R}_2 - \mathbf{r}|} + V_{\mathrm{H}}(\mathbf{r}) + V_{\mathrm{x}\sigma}^{\mathrm{KLI}}(\mathbf{r}) \right) \varphi_{j\sigma}(\mathbf{r}) = \varepsilon_{j\sigma}\varphi_{j\sigma}(\mathbf{r}), \quad (29)
$$

where $\mathbf{R_i}$ denotes the location and Z_i the nuclear charge of the i-th nucleus in the molecule. The partial differential equation is solved in prolate spheroidal coordinates on a two-dimensional mesh by a relaxation method, while the third variable, the azimuthal angle, is treated analytically. The Hartree potential

$$
V_{\mathrm{H}}(\mathbf{r}) = \int d^3 r' \, \frac{\rho(\mathbf{r}')}{|\mathbf{r} - \mathbf{r}'|} \tag{30}
$$

and the functions $u_{\mathrm{x}i\sigma}(\mathbf{r})$ (cf. Eq. (21)) needed for the calculation of the exchange potential $V_{\mathrm{x}\sigma}^{\mathrm{KLI}}(\mathbf{r})$ (cf. Eq. (24)) are computed as solutions of a Poisson and Poisson-like equation, respectively. In this step, the same relaxation technique as for the solution of the Schrödinger equation (29) is employed. Starting with an initial guess for the wave functions $\varphi_{i\sigma}(\mathbf{r})$, equations (29), (30), (21) together with (24) are iterated until self-consistent. A very detailed description of the code is given in [24].

In order to test the accuracy of the program, we have performed calculations on the Beryllium and Neon atom which are compared in Table 1 to exact results obtained with a one-dimensional atomic code. The results agree to all decimals given. Furthermore, from Table 2 it is evident that our program gives results for the two-electron molecules He$_2$ and HeH$^+$ which are identical to the HF ones obtained by Laaksonen et al [22] as they should be, as the HF and x-only KLI schemes are identical for these systems.

For comparison, we have performed additional x-only calculations with two other approximations of $V_{x\sigma}(\mathbf{r})$ and E_x, respectively. The first one of these, denoted by *Slater* in the following, uses - like the HF and x-only KLI method - the exact orbital representation of E_x given in equation (20) but the averaged exchange potential due to Slater [25] given by

$$
V_{x\sigma}^{S}(\mathbf{r}) = -\frac{1}{\rho_\sigma(\mathbf{r})} \sum_{i,j=1}^{N_\sigma} \varphi_{j\sigma}^*(\mathbf{r})\varphi_{i\sigma}(\mathbf{r}) \int d^3 r' \, \frac{\varphi_{i\sigma}^*(\mathbf{r}')\varphi_{j\sigma}(\mathbf{r}')}{|\mathbf{r} - \mathbf{r}'|}, \tag{31}
$$

which may be obtained from (24) by setting the constants $\bar{V}_{\mathrm{xc}i\sigma} - \bar{u}_{\mathrm{xc}i\sigma}$ equal to zero for all i. The other is the well known x-only local density approximation (LDA) of conventional DFT. As for the KLI calculations, we have successfully tested our implementations on atomic systems.

	Beryllium		Neon	
	1D	2D	1D	2D
Grid	400	153×249	400	153×249
E_{TOT}	-14.5723	-14.5723	-128.5448	-128.5448
ε_{HOMO}	-0.3089	-0.3089	-0.8494	-0.8494
$< 1/r >$	2.1039	2.1039	3.1100	3.1100
$< r^2 >$	4.3255	4.3255	0.9367	0.9367

Table 1: X-only KLI results for the Beryllium and Neon atom. 1D denotes exact values obtained with our one-dimensional code, 2D the results from our two-dimensional code with one nuclear charge set equal to zero. All numbers in atomic units.

	H_2		HeH^+	
R	1.4		1.455	
	HF	x-only KLI	HF	x-only KLI
E_{TOT}	-1.133630	-1.133630	-2.933103	-2.933103
$\varepsilon_{1\sigma}$	-0.594659	-0.594659	-1.637451	-1.637451
Q_1^e	0	0	-0.494460	-0.494460
Q_2^e	0.243289	0.243289	0.373727	0.373727
Q_3^e	0	0	-0.231525	-0.231525
Q_4^e	0.090721	0.090721	0.173962	0.173962
$< r^2 >$	2.573930	2.573930	1.340832	1.340832

Table 2: Comparison of results for two electron molecules with assumed bond length R. HF values from [22]. Q_1^e, Q_2^e, Q_3^e, Q_4^e, denote the electronic contributions to the dipole, quadrupole, octopole and hexadecapole moments per electron, respectively, determined from the molecular midpoint. All numbers in atomic units.

	HF	x-only KLI	Slater	x-only LDA
E_{TOT}	-7.9874	-7.9868	-7.9811	-7.7043
$\varepsilon_{1\sigma}$	-2.4452	-2.0786	-2.3977	-1.7786
$\varepsilon_{2\sigma}$	-0.3017	-0.3011	-0.3150	-0.1284
Q_1^e	0.6531	0.6440	0.8614	0.8679
Q_2^e	7.1282	7.1365	6.9657	6.7717
Q_3^e	2.9096	2.9293	3.0799	2.6924
Q_4^e	16.0276	16.1311	15.5881	15.0789

Table 3: X-only results for LiH. HF values for bond length of 3.015 a.u. from [24]. Present calculations performed on a 153×193 grid with bond length of 3.015 a.u. All numbers in atomic units.

	HF	x-only KLI	Slater	x-only LDA
E_{TOT}	-25.1316	-25.1290	-25.1072	-24.6299
$\varepsilon_{1\sigma}$	-7.6863	-6.8624	-7.4837	-6.4715
$\varepsilon_{2\sigma}$	-0.6482	-0.5856	-0.6358	-0.3956
$\varepsilon_{3\sigma}$	-0.3484	-0.3462	-0.3721	-0.1626
Q_1^e	5.3525	5.3498	5.2991	5.3154
Q_2^e	12.1862	12.1416	11.4720	11.9542
Q_3^e	15.6411	15.5618	14.3328	14.0904
Q_4^e	25.8492	25.4188	25.2152	21.9134

Table 4: X-only results for BH. HF values for bond length of 2.336 a.u. from [24]. Present calculations performed on a 193×265 grid with bond length of 2.336 a.u. All numbers in atomic units.

	HF	x-only KLI	Slater	x-only LDA
E_{TOT}	-100.0708	-100.0675	-100.0225	-99.1512
$\varepsilon_{1\sigma}$	-26.2946	-24.5116	-25.6625	-24.0209
$\varepsilon_{2\sigma}$	-1.6010	-1.3994	-1.4327	-1.0448
$\varepsilon_{3\sigma}$	-0.7682	-0.7772	-0.8167	-0.4483
$\varepsilon_{1\pi}$	-0.6504	-0.6453	-0.6897	-0.3109
Q_1^{tot}	-0.7561	-0.8217	-0.8502	-0.6962
Q_2^{tot}	1.7321	1.8013	1.8472	1.7124
Q_3^{tot}	-2.5924	-2.7222	-2.8782	-2.4662
Q_4^{tot}	5.0188	5.1825	5.3720	4.7068
$< 1/r >_H$	6.1130	6.0878	6.0909	6.0901
$< 1/r >_F$	27.1682	27.1622	27.6049	27.0289

Table 5: X-only results for FH. HF values for bond length of 1.7328 a.u. from [24]. Present calculations performed on a 161×321 grid with bond length of 1.7328 a.u. All numbers in atomic units.

	HF	x-only KLI	Slater	x-only LDA
E_{TOT}	-5.72333	-5.72332	-5.72332	-5.44740
$\varepsilon_{1\sigma g}$	-0.92017	-0.91929	-0.91977	-0.51970
$\varepsilon_{1\sigma u}$	-0.91570	-0.91566	-0.91614	-0.51452
Q_2^e	31.36165	31.35931	31.35907	31.35507
Q_4^e	245.8779	245.8643	245.8615	245.8255

Table 6: X-only results for He_2. HF values for bond length of 5.6 a.u. from [24]. Present calculations performed on a 209×225 grid with bond length of 5.6 a.u. All numbers in atomic units.

	HF	x-only KLI	Slater	x-only LDA
E_{TOT}	-14.8716	-14.8706	-14.8544	-14.3970
$\varepsilon_{1\sigma g}$	-2.4531	-2.0276	-2.3875	-1.7869
$\varepsilon_{1\sigma u}$	-2.4528	-2.0272	-2.3873	-1.7864
$\varepsilon_{2\sigma g}$	-0.1820	-0.1813	-0.1989	-0.0922
Q_2^e	27.6362	27.4993	29.0014	29.4401
Q_4^e	159.9924	159.6809	169.1300	172.8505

Table 7: X-only results for Li_2. HF values for bond length of 5.051 a.u. from [24]. Present calculations performed on a 209×225 grid with bond length of 5.051 a.u. All numbers in atomic units.

	HF	x-only KLI	Slater	x-only LDA
E_{TOT}	-29.1337	-29.1274	-29.0939	-28.4612
$\varepsilon_{1\sigma g}$	-4.73150	-4.09876	-4.60353	-3.78576
$\varepsilon_{1\sigma u}$	-4.73147	-4.09872	-4.60351	-3.87571
$\varepsilon_{2\sigma g}$	-0.39727	-0.33452	-0.37659	-0.23067
$\varepsilon_{2\sigma u}$	-0.24209	-0.23489	-0.26524	-0.13163
Q_2^e	46.0878	46.2475	43.4833	46.2501
Q_4^e	261.774	277.365	249.135	281.950

Table 8: X-only results for Be_2. HF values for bond length of 4.6 a.u. from [24]. Present calculations performed on a 209×225 grid with bond length of 4.6 a.u. All numbers in atomic units.

	HF	x-only KLI	Slater	x-only LDA
E_{TOT}	-108.9936	-108.9856	-108.9110	-107.7560
$\varepsilon_{1\sigma g}$	-15.6822	-14.3722	-15.2692	-13.8950
$\varepsilon_{1\sigma u}$	-15.6787	-14.3709	-15.2682	-13.8936
$\varepsilon_{2\sigma g}$	-1.4726	-1.3076	-1.3316	-0.9875
$\varepsilon_{2\sigma u}$	-0.7784	-0.7453	-0.7473	-0.4434
$\varepsilon_{3\sigma g}$	-0.6347	-0.6305	-0.6521	-0.3335
$\varepsilon_{1\pi u}$	-0.6152	-0.6818	-0.6960	-0.3887
Q_2^{tot}	-0.9372	-0.9488	-1.1756	-1.1643
Q_4^{tot}	-7.3978	-6.7476	-7.1266	-6.2553
$< 1/r >_N$	21.6543	21.6439	21.9749	21.5820

Table 9: X-only results for N_2. HF values for bond length of 2.07 a.u. from [24]. Present calculations performed on a 209×225 grid with bond length of 2.07 a.u. All numbers in atomic units.

Results are given in Tables 3 through 9 for LiH, BH, FH, He_2, Li_2, Be_2 and N_2. For each system we show the total ground state energy E_{TOT}, the various orbital energy eigenvalues ε and the nonzero electronic contributions to the dipole, quadrupole, octopole and hexadecapole moments denoted by Q_1^e, Q_2^e, Q_3^e and Q_4^e calculated from the geometrical center of the molecule, respectively, except for FH and N_2, where the total moments (including nuclear contributions) calculated from the center of mass are given, denoted by Q_L^{tot}. For these two molecules we also present the expectation values of $1/r$, denoted by $< 1/r >$, calculated at the nuclei.

For all physical quantities of interest, i.e. for E_{TOT}, the energies ε_{HOMO} of the highest occupied orbitals and the multipole moments, the x-only KLI and HF results differ only slightly, usually by a few hundredths of a percent for total energies, a few tenths of a percent for ε_{HOMO} and a few percent for the multipole moments. The largest difference between the ε_{HOMO} values occurs for Be_2, where they differ by 3%. For N_2, the energetic order of the $1\pi_u$ and $3\sigma_g$ orbital is reversed in all DFT approaches as compared to the HF result, which corresponds to the experimentally observed order of the outer valence ionization potentials [26]. As far as the multipole moments are concerned, the largest discrepancy between the x-only KLI and HF approaches occurs for the total hexadecapole moment of N_2, where the results differ by 8.8%. In this case, the Slater approximation gives a value differing only by 3.7% from the HF one. The $1/r$ expectation values obtained with the HF and x-only KLI method are almost identical, differing by only a few hundreths of a precent with the exception of the one for the Hydrogen nucleus in FH, where the difference is an order of magnitude larger. In this case, both the Slater as well as the x-only LDA approximations give values closer to the HF results.

The Slater method gives - with a few exceptions mentioned above - values for E_{TOT}, ε_{HOMO}, the multipole moments and $1/r$ expectation values which differ to a larger extent from both the KLI and HF results than the latter from each other. From the energy eigenvalues of the inner orbitals, on the other hand, it is obvious that the Slater exchange potential $V_{x\sigma}^S(\mathbf{r})$ is deeper than the one obtained in the KLI method, giving results closer the HF ones.

Finally, the x-only LDA results differ more strongly from the other methods, yielding much higher total energies. The difference is most pronounced for the values of ε_{HOMO}, which are roughly twice as large as the ones from any of the other methods. This is due to the wrong exponential decay of $V_{x\sigma}^{LDA}(\mathbf{r})$ for large r.

We point out that the bulk part of the difference between the x-only KLI and the HF results are not due to the KLI approximation, but to the different nature of the HF and the DFT approaches. This is an established fact for atomic systems [9, 10, 11] and we see no reason why it should not hold for molecular systems as well. We mention that the difference between the HF and the exact x-only DFT results also implies that the *exact* quantum chemical correlation energy and the *exact* DFT correlation energy are not identical [27].

4 Correlation contributions to the OEP

The inclusion of correlation effects into the OEP scheme is straightforward, as anticipated by the indices xc in section 2, once an explicit functional for $E_c[\{\varphi_{j\tau}\}]$ has been specified. It has been shown [15, 27] that the orbital-dependent Colle-Salvetti functional [28, 29] is well suited for this purpose. It yields excellent results for atoms, surpassing the accurracy of conventional Kohn-Sham calculations. In this approximation, E_c is given by [15]

$$
\begin{aligned}
E_c[\{\varphi_{j\tau}\}] \;=\; & -ab \int d^3r \; \gamma(\mathbf{r})\xi(\mathbf{r})\left[\sum_\sigma \rho_\sigma(\mathbf{r}) \sum_i |\nabla\varphi_{i\sigma}(\mathbf{r})|^2 \;-\; \frac{1}{4}|\nabla\rho(\mathbf{r})|^2 \right.\\
& \left. -\frac{1}{4}\sum_\sigma \rho_\sigma(\mathbf{r})\triangle\rho_\sigma(\mathbf{r}) \;+\; \frac{1}{4}\rho(\mathbf{r})\triangle\rho(\mathbf{r}) \right] \\
& -a \int d^3r \; \gamma(\mathbf{r})\frac{\rho(\mathbf{r})}{\eta(\mathbf{r})},
\end{aligned}
\tag{32}
$$

where

$$
\gamma(\mathbf{r}) \;=\; 4\,\frac{\rho_\uparrow(\mathbf{r})\rho_\downarrow(\mathbf{r})}{\rho(\mathbf{r})^2},
\tag{33}
$$

$$
\eta(\mathbf{r}) \;=\; 1 + d\rho(\mathbf{r})^{-\frac{1}{3}},
\tag{34}
$$

$$
\xi(\mathbf{r}) \;=\; \frac{\rho(\mathbf{r})^{-\frac{5}{3}}e^{-c\rho(\mathbf{r})^{-\frac{1}{3}}}}{\eta(\mathbf{r})}
\tag{35}
$$

and

$$
\begin{aligned}
a &= 0.04918, & b &= 0.132, \\
c &= 0.2533, & d &= 0.349.
\end{aligned}
$$

4.1 Two-Electron Systems

In order to study the correlation contributions more thoroughly, we first concentrate on two-electron atoms for two reasons. First of all, as pointed out above, the solution of the full OEP integral equation for these systems is identical to the one obtained from the KLI-scheme. As the exchange energy functional is also known exactly, c.f. equation (20), the only error made is due to the approximation for E_c. Secondly there exist practically exact solutions [31] of the two-particle Schrödinger equation so that various DFT-related quantities of interest can be compared with exact results.

In Table 10 we show the total absolute ground-state energies of the atoms isoelectronic with helium. The first column, denoted by KLICS, displays the results obtained with the above described method, including the Colle-Salvetti functional for E_c into the OEP scheme. The next two columns show results obtained with the conventional Kohn-Sham method for comparison. BLYP denotes the use of the exchange-energy functional by Becke [32] combined with the correlation energy functional by Lee, Yang and Parr [33], whereas the third column headed PW91 refers to the generalized gradient approximation by Perdew and Wang [34]. The exact nonrelativistic results in the last column are taken from [30]. Note that there

	KLICS	BLYP	PW91	exact
H^-	0.5189			0.5278
He	2.9033	2.9071	2.9000	2.9037
Li^+	7.2803	7.2794	7.2676	7.2799
Be^{2+}	13.6556	13.6500	13.6340	13.6556
B^{3+}	22.0301	22.0200	21.9996	22.0310
C^{4+}	32.4045	32.3896	32.3649	32.4062
N^{5+}	44.7788	44.7592	44.7299	44.7814
O^{6+}	59.1531	59.1286	59.0948	59.1566
F^{7+}	75.5274	75.4981	75.4595	75.5317
Ne^{8+}	93.9017	93.8675	93.8241	93.9068
Na^{9+}	114.2761	114.2369	114.1886	114.2819
Mg^{10+}	136.6505	136.6064	136.5531	136.6569
Al^{11+}	161.0250	160.9758	160.9175	161.0320
Si^{12+}	187.3995	187.3453	187.2819	187.4070
P^{13+}	215.7740	215.7147	215.6462	215.7821
S^{14+}	246.1485	246.0842	246.0105	246.1571
Cl^{15+}	278.5231	278.4536	278.3748	278.5322
Ar^{16+}	312.8977	312.8231	312.7390	312.9072
K^{17+}	349.2723	349.1926	349.1032	349.2822
Ca^{18+}	387.6470	387.5620	387.4674	387.6572
$\triangle$	0.0053	0.0450	0.0943	

Table 10: Total absolute ground-state energies for the Helium isoelectronic series from various self-consistent calculations. $\triangle$ denotes the mean absolute deviation from the exact values from [30] . All numbers in atomic units.

is no convergence for neagtive ions in the conventional Kohn Sham method. All of our calculations have been performed with a basis-set-free, fully numerical atomic code which solves the radial Schrödinger equation (1) by the Numerov-method as described in [35]. The angular parts are treated analytically.

In Figure 1, we have plotted the errors $E_{tot}^{DFT} - E_{tot}^{exact}$ of the numbers shown in Table 10. It is obvious that the KLICS scheme gives superior results. The mean absolute error, denoted by $\triangle$, is smaller by an order of magnitude for the KLICS results as compared to the two conventional Kohn Sham approaches. This comes as no surprise, as the exchange part is treated exactly in the OEP method, whereas only approximative functionals can be used in the Kohn-Shame scheme. As may be read off Table 11, where we show the exchange and correlation contributions to the total energy seperately for systems where exact values are available, an error cancellation occurs in the BLYP and PW91 approaches - the exchange energies being too large and the correlation energies being to small in magnitude. The KLICS results for these two quantities are clearly much better. However, for the highly charged two-electron ions the quality of the results decreases substantially in all approaches. For these systems the LYP-functional appears to perform best.

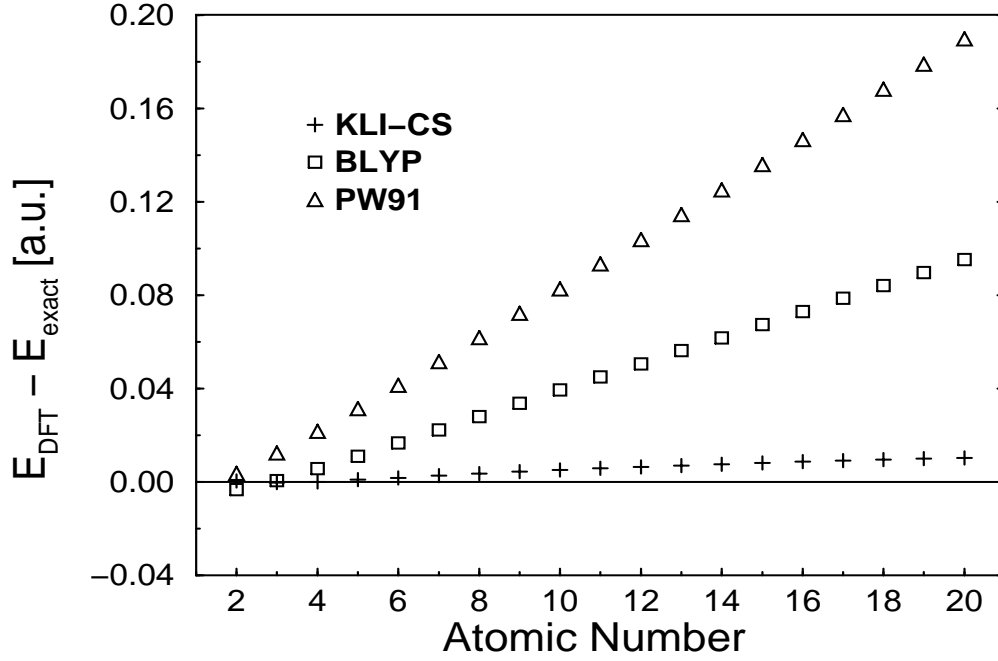In order to assess the quality of the xc potentials resulting from various approx-

Figure 1: Energy differences corresponding to Table 10

	element	KLICS	BLYP	PW91	exact
	H^-	0.4053			0.3809
	He	1.0275	1.0183	1.0095	1.0246
$-E_x$	Be^{2+}	2.2768	2.2573	2.2367	2.2766
	Ne^{8+}	6.0272	5.9749	5.9189	6.0275
	Hg^{78+}	49.7779	49.3412	48.8806	49.7779
	H^-	0.0312			0.0420
	He	0.0416	0.0437	0.0450	0.0421
$-E_c$	Be^{2+}	0.0442	0.0493	0.0530	0.0443
	Ne^{8+}	0.0406	0.0504	0.0615	0.0457
	Hg^{78+}	0.0276	0.0506	0.0805	0.0465

Table 11: Exchange and correlation energies from various approximations. Exact values from [31]. All values in atomic units.

imate functionals, it is informative to look at the highest occupied orbital energy of the system. In an *exact* implementation of DFT this value should be equal to the ionization potential of the system. Therefore, the resulting values from *approximate* schemes are an indication of the quality of the corresponding xc potential. From Table 12, where we have listed these numbers for various self-consistent approximations together with the exact ones, it is obvious that the KLICS scheme performs much better than the conventional Kohn-Sham schemes. The difference is less pronounced for the highly charged ions as the nuclear potential becomes the dominant term in the Kohn-Sham potential (3). A glance at the second column, in which we give the corresponding values from an *x-only* KLI calculation, shows, however, that the reason for the superior quality is due to the inclusion of the exact exchange in the KLI scheme, which results in the correct $-1/r$ asymptotic behaviour of the xc potential. In fact, adding the Colle-Salvetti formula for the correlation energy slightly worsens the results, as may be seen by comparing the second and third columns: The correlation contribution lowers the already too small values from the x-only calculations for the highest occupied orbital energy even more.

	KLI	KLICS	BLYP	PW91	exact
	x-only	xc	xc	xc	
He	0.9180	0.9446	0.5849	0.5833	0.9037
Li^+	2.7924	2.8227	2.2312	2.2269	2.7799
Be^{2+}	5.6671	5.6992	4.8760	4.8701	5.6556
B^{3+}	9.5420	9.5751	8.5201	8.5129	9.5310
C^{4+}	14.4169	14.4507	13.1638	13.1554	14.4062
N^{5+}	20.2918	20.3261	18.8072	18.7978	20.2814
O^{6+}	27.1668	27.2014	25.4504	25.4401	27.1566
F^{7+}	35.0418	35.0766	33.0935	33.0823	35.0317
Ne^{8+}	43.9167	43.9517	41.7366	41.7245	43.9068
Na^{9+}	53.7917	53.8269	51.3796	51.3666	53.7819
Mg^{10+}	64.6667	64.7020	62.0225	62.0086	64.6569
Al^{11+}	76.5417	76.5770	73.6654	73.6506	76.5320
Si^{12+}	89.4167	89.4521	86.3083	86.2926	89.4071
P^{13+}	103.2917	103.3272	99.9511	99.9345	103.2821
S^{14+}	118.1666	118.2022	114.5939	114.5764	118.1571
Cl^{15+}	134.0416	134.0773	130.2367	130.2183	134.0322
Ar^{16+}	150.9166	150.9523	146.8795	146.8602	150.9072
K^{17+}	168.7916	168.8273	164.5223	164.5021	168.7822
Ca^{18+}	187.6666	187.7024	183.1650	183.1439	187.6572

Table 12: Absolute highest occupied orbital energies from various self-consistent calculations. Exact values calculated from [30]. All values in atomic units.

The error in the correlation potential responsible for this behaviour is clearly visible from Figure 2 where we plot the exact [31] and various self-consistent correlation potentials. The potential obtained with the Colle-Salvetti functional within
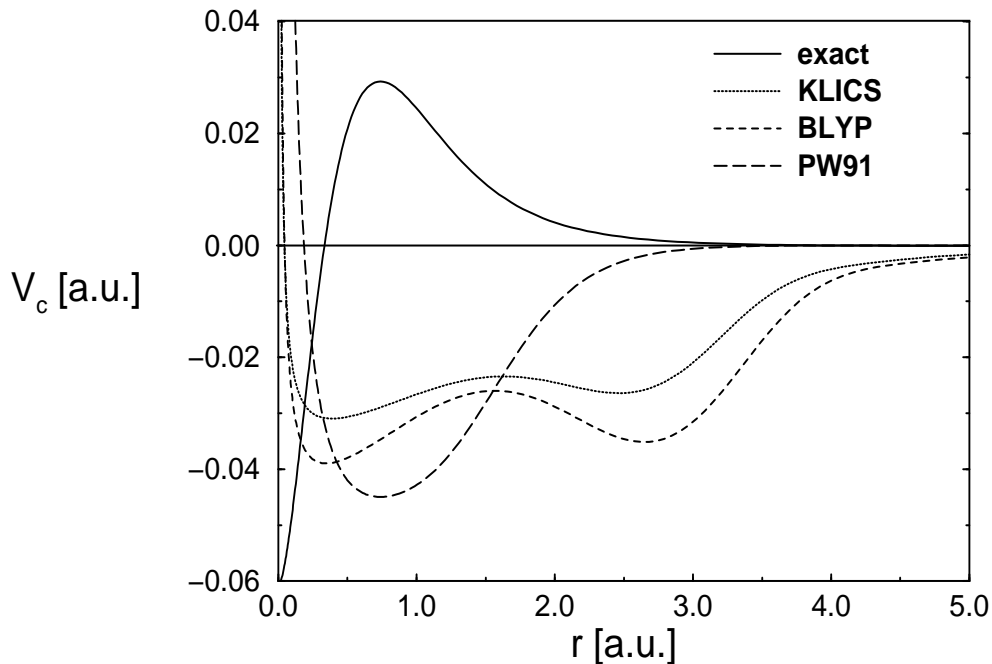
Figure 2: Comparison of the exact and self-consistently calculated correlation potentials of helium

the KLICS scheme shows the same deficiencies as the conventional density functionals: Instead of a maximum with positive values of the potential, the approximations possess one or even two minima and spurious divergences occur at the origin, which may be traced back to gradients of the density and of the one-particle orbitals occuring in the various correlation energy functionals. The need for further improvement of the correlation energy functional in this respect is obvious.

4.2   Beryllium and Neon Isoelectronic Series

For further analysis we have calculated the total ground state energies of positive ions isoelectronic with Beryllium (shown in Table 13) and Neon (shown in Table 14). Again, we compare the various DFT methods with exact data from Ref. [36]. The errors are plotted in Figures 3 and 4, respectively. The data for both series show the same trends: The overall best results are obtained with the KLICS scheme, where the absolute mean deviation $\triangle$ from the exact values is smallest. The BLYP scheme is only slightly worse, but the PW91 functional gives errors which are roughly twice as large as compared to the other DFT approaches. From the plots in Figures 3 and 4 it is obvious that these statements hold for most ions individually.

There are two other trends to be noted in these results. First we point out that although the absolute errors rise within the isoelectronic series as the atomic number increases, the percentage errors remain almost constant. And secondly, the mean absolute error is smaller by almost an order of magnitude for the ten-electron series compared to the four-electron series.

15

	KLICS	BLYP	PW91	exact
Be	14.6651	14.6615	14.6479	14.6674
B^+	24.3427	24.3366	24.3160	24.3489
C^{2+}	36.5224	36.5143	36.4881	36.5349
N^{3+}	51.2025	51.1927	51.1618	51.2228
O^{4+}	68.3825	68.3713	68.3362	68.4117
F^{5+}	88.0624	88.0499	88.0110	88.1011
Ne^{6+}	110.2420	110.2285	110.1859	110.2909
Na^{7+}	134.9216	134.9071	134.8610	134.9809
Mg^{8+}	162.1010	162.0857	162.0361	162.1710
Al^{9+}	191.7803	191.7642	191.7113	191.8613
Si^{10+}	223.9595	223.9427	223.8864	224.0516
P^{11+}	258.6387	258.6212	258.5616	258.7420
S^{12+}	295.8178	295.7996	295.7367	295.9324
Cl^{13+}	335.4968	335.4781	335.4119	335.6229
Ar^{14+}	377.6758	377.6566	377.5870	377.8134
K^{15+}	422.3548	422.3350	422.2621	422.5040
Ca^{16+}	469.5338	469.5134	469.4372	469.6946
Sc^{17+}	519.2127	519.1919	519.1122	519.3851
Ti^{18+}	571.3917	571.3703	571.2873	571.5757
V^{19+}	626.0706	626.0487	625.9623	626.2663
Cr^{20+}	683.2495	683.2271	683.1373	683.4570
Mn^{21+}	742.9284	742.9056	742.8123	743.1476
Fe^{22+}	805.1072	805.0840	804.9873	805.3382
Co^{23+}	869.7861	869.7624	869.6623	870.0289
Ni^{24+}	936.9650	936.9408	936.8373	937.2195
$\triangle$	0.1180	0.1352	0.1973	

Table 13: Total absolute ground-state energies for the Beryllium isoelectronic series from various self-consistent calculations. $\triangle$ denotes the mean absolute deviation from the exact values from [36] . All numbers in atomic units.

The ionization potentials from the various approaches as calculated from the highest occupied Kohn-Sham orbitals are shown in Tables 15 and 16 for the four- and ten-electron series, respectively. The exact nonrelativistic values have been calculated from the data given in [36]. Due to the correct asymptotic behaviour of the xc-potential for large r within the OEP scheme it comes as no surprise that the KLICS data are superior to the conventional Kohn-Sham approach. The effect of the correlation potential within the OEP scheme is – like in the two-electron case – a lowering of the energy eigenvalue of the highest occupied orbital, as may be seen from a comparison of the second and third columns showing the OEP results in x-only approximation and with inclusion of correlation in the form of Colle-Salvetti in the KLI-scheme, respectively. As opposed to the Helium and Neon isoelectronic series, this effect improves the quality of the results in the Beryllium isoelectronic series. We mention that the ionization potentials are in much better agreement

	KLICS	BLYP	PW91	exact
Ne	128.9202	128.9730	128.9466	128.9376
Na^+	162.0645	162.0956	162.0668	162.0659
Mg^{2+}	199.2291	199.2448	199.2136	199.2204
Al^{3+}	240.4071	240.4102	240.3768	240.3914
Si^{4+}	285.5945	285.5867	285.5509	285.5738
P^{5+}	334.7888	334.7712	334.7331	334.7642
S^{6+}	387.9885	387.9616	387.9212	387.9608
Cl^{7+}	445.1922	445.1567	445.1138	445.1622
Ar^{8+}	506.3993	506.3554	506.3101	506.3673
K^{9+}	571.6091	571.5570	571.5092	571.5754
Ca^{10+}	640.8211	640.7610	640.7107	640.7861
Sc^{11+}	714.0350	713.9671	713.9141	713.9988
Ti^{12+}	791.2504	791.1748	791.1191	791.2132
V^{13+}	872.4671	872.3839	872.3255	872.4291
Cr^{14+}	957.6850	957.5942	957.5331	957.6463
Mn^{15+}	1046.9039	1046.8056	1046.7417	1046.8646
Fe^{16+}	1140.1237	1140.0179	1139.9511	1140.0838
Co^{17+}	1237.3442	1237.2309	1237.1613	1237.3039
Ni^{18+}	1338.5654	1338.4447	1338.3722	1338.5247
$\triangle$	0.0293	0.0334	0.0694	

Table 14: Total absolute ground-state energies for the Neon isoelectronic series from various self-consistent calculations. $\triangle$ denotes the mean absolute deviation from the exact values from [36] . All numbers in atomic units.
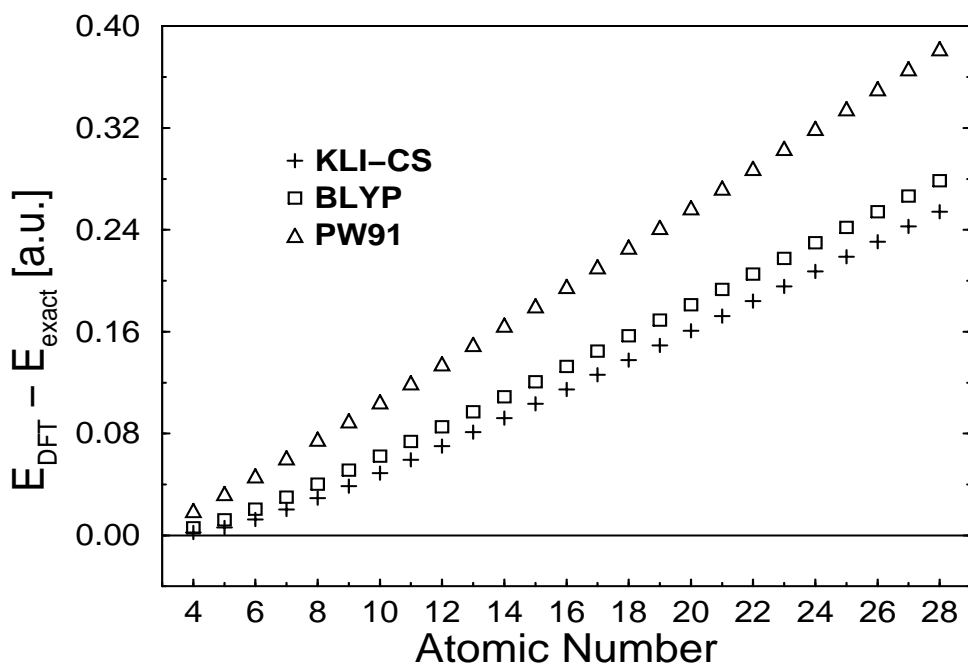with the exact results if they are calculated as ground-state energy differences [15].

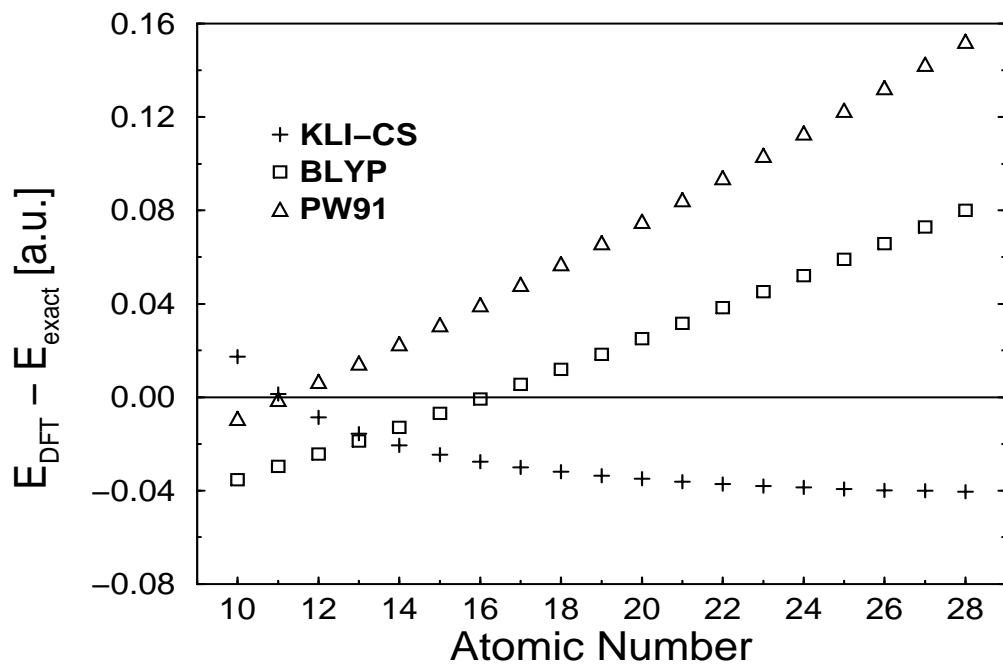Figure 3: Energy differences corresponding to Table 13.

Figure 4: Energy differences corresponding to Table 14

	KLI x-only	KLICS xc	BLYP xc	PW91 xc	exact
Be	0.3089	0.3294	0.2009	0.2072	0.3426
B^+	0.8732	0.8992	0.7129	0.7185	0.9243
C^{2+}	1.6933	1.7226	1.4804	1.4856	1.7594
N^{3+}	2.7659	2.7975	2.5000	2.5049	2.8459
O^{4+}	4.0898	4.1231	3.7706	3.7754	4.1832
F^{5+}	5.6644	5.6991	5.2918	5.2964	5.7708
Ne^{6+}	7.4896	7.5253	7.0633	7.0678	7.6087
Na^{7+}	9.5652	9.6017	9.0850	9.0894	9.6967
Mg^{8+}	11.8910	11.9281	11.3569	11.3611	12.0348
Al^{9+}	14.4669	14.5047	13.8788	13.8829	14.6230
Si^{10+}	17.2930	17.3312	16.6508	16.6548	17.4613
P^{11+}	20.3692	20.4078	19.6729	19.6768	20.5496
S^{12+}	23.6955	23.7345	22.9450	22.9487	23.8880
Cl^{13+}	27.2718	27.3111	26.4671	26.4707	27.4763
Ar^{14+}	31.0982	31.1378	30.2393	30.2427	31.3147
K^{15+}	35.1747	35.2145	34.2615	34.2647	35.4031
Ca^{16+}	39.5012	39.5412	38.5336	38.5367	39.7416
Sc^{17+}	44.0777	44.1179	43.0558	43.0587	44.3300
Ti^{18+}	48.9043	48.9447	47.8280	47.8307	49.1684
V^{19+}	53.9808	54.0214	52.8502	52.8527	54.2569
Cr^{20+}	59.3074	59.3481	58.1224	58.1247	59.5954
Mn^{21+}	64.8840	64.9249	63.6447	63.6467	65.1838
Fe^{22+}	70.7107	70.7516	69.4169	69.4187	71.0223
Co^{23+}	76.7873	76.8284	75.4391	75.4408	77.1108
Ni^{24+}	83.1140	83.1551	81.7113	81.7128	83.4493

Table 15: Ionization potentials from highest occupied Kohn-Sham orbital energies for the Beryllium isoelectronic series from various self-consistent calculations. Exact nonrelativistic values calculated from [36] . All numbers in atomic units.

	KLI	KLICS	BLYP	PW91	exact
	x-only	xc	xc	xc	
Ne	0.8494	0.8841	0.4914	0.4942	0.7945
Na^+	1.7959	1.8340	1.3377	1.3416	1.7410
Mg^{2+}	3.0047	3.0450	2.4531	2.4579	2.9499
Al^{3+}	4.4706	4.5125	3.8285	3.8339	4.4161
Si^{4+}	6.1912	6.2343	5.4601	5.4661	6.1371
P^{5+}	8.1651	8.2091	7.3458	7.3524	8.1112
S^{6+}	10.3914	10.4362	9.4846	9.4917	10.3378
Cl^{7+}	12.8696	12.9150	11.8757	11.8832	12.8162
Ar^{8+}	15.5992	15.6451	14.5185	14.5264	15.5460
K^{9+}	18.5800	18.6263	17.4126	17.4209	18.5270
Ca^{10+}	21.8118	21.8585	20.5579	20.5665	21.7589
Sc^{11+}	25.2943	25.3413	23.9541	23.9630	25.2416
Ti^{12+}	29.0274	29.0747	27.6010	27.6102	28.9748
V^{13+}	33.0112	33.0587	31.4986	31.5080	32.9586
Cr^{14+}	37.2453	37.2931	35.6467	35.6563	37.1929
Mn^{15+}	41.7299	41.7779	40.0453	40.0551	41.6776
Fe^{16+}	46.4649	46.5130	44.6943	44.7042	46.4126
Co^{17+}	51.4501	51.4984	49.5936	49.6037	51.3979
Ni^{18+}	56.6856	56.7341	54.7432	54.7535	56.6335

Table 16: Ionization potentials from highest occupied Kohn-Sham orbital energies for the Neon isoelectronic series from various self-consistent calculations. Exact nonrelativistic values calculated from [36] . All numbers in atomic units.

5 Conclusions

Our calculations for molecular systems reveal that the KLI approach is also feasible for more complex systems and gives results of similar quality as for atoms. We expect that an inclusion of correlation effects will result in a highly accurate DFT scheme. The studies of correlation contributions to atomic systems show that further improvement of the presently available correlation-energy functionals is necessary.

6 Acknowledgments

References

[1] J.D. Talman and W.F. Shadwick, Phys. Rev. A **14**, 36 (1976).

[2] R.T. Sharp and G.K. Horton, Phys. Rev. **90**, 317 (1953).

[3] V. Sahni, J. Gruenebaum, and J.P. Perdew, Phys. Rev. B **26**, 4371 (1982).

[4] J.P. Perdew and M.R. Norman, Phys. Rev. B **26**, 5445 (1982).

[5] P. Hohenberg and W. Kohn, Phys. Rev. **136**, B864 (1964).

[6] W. Kohn and L.J. Sham, Phys. Rev. **140**, A1133 (1965).

[7] R.M. Dreizler and E.K.U. Gross, *Density Functional Theory* (Springer, Berlin, 1990).

[8] R.G. Parr and W. Yang, *Density-Functional Theory of Atoms and Molecules* (Oxford University Press, New York, 1989).

[9] J.B. Krieger, Y. Li, and G.J. Iafrate, Phys. Rev. A **45**, 101 (1992).

[10] J.B. Krieger, Y. Li, and G.J. Iafrate, Phys. Rev. A **46**, 5453 (1992).

[11] Y. Li, J.B. Krieger, and G.J. Iafrate, Phys. Rev. A **47**, 165 (1993).

[12] U. von Barth and L. Hedin, J. Phys. C **5**, 1629 (1972).

[13] M.M. Pant and A.K. Rajagopal, Sol. State Commun. **10**, 1157 (1972).

[14] A. Görling and M. Levy, Phys. Rev. A **50**, 196 (1994).

[15] T. Grabo and E.K.U. Gross, Chem. Phys. Lett. **240**, 141 (1995).

[16] M.R. Norman and D.D. Koelling, Phys. Rev. B **30**, 5530 (1984).

[17] Y. Wang, J.P. Perdew, J.A. Chevary, L.D. Macdonald, and S.H. Vosko, Phys. Rev. A **41**, 78 (1990).

[18] E. Engel, J.A. Chevary, L.D. Macdonald, and S.H. Vosko, Z. Phys. D **23**, 7 (1992).

[19] E. Engel and S.H. Vosko, Phys. Rev. A **47**, 2800 (1993).

[20] J.B. Krieger, Y. Li, and G.J. Iafrate, in *Density Functional Theory*, edited by R.M. Dreizler and E.K.U. Gross (Plenum Press, New York, 1995).

[21] L. Laaksonen, P. Pyykkö, and D. Sundholm, Int. J. Quantum Chem. **23**, 309 (1983).

[22] L. Laaksonen, P. Pyykkö, and D. Sundholm, Int. J. Quantum Chem. **23**, 319 (1983).

[23] L. Laaksonen, D. Sundholm, and P. Pyykkö, Int. J. Quantum Chem. **28**, 601 (1985).

[24] L. Laaksonen, P. Pyykkö, and D. Sundholm, Comp. Phys. Reports **4**, 313 (1986).

[25] J.C. Slater, Phys. Rev. **81**, 385 (1951).

[26] C. Jamorski, M.E. Casida, and D.R. Salahub, J. Chem. Phys. **104**, 5134 (1996).

[27] E.K.U. Gross, M. Petersilka, and T. Grabo, in *Chemical Applications of Density Functional Theory, ACS Symposium Series 629*, edited by B.B Laird, R.B. Ross, and T. Ziegler (American Chemical Society, Washington, DC, 1996).

[28] R. Colle and D. Salvetti, Theoret. Chim. Acta **37**, 329 (1975).

[29] R. Colle and D. Salvetti, Theoret. Chim. Acta **53**, 55 (1979).

[30] E.R. Davidson, S.A. Hagstrom, S.J. Chakravorty, V.M. Umar, and C. Froese Fischer, Phys. Rev. A **44**, 7071 (1991).

[31] C.J. Umrigar and X. Gonze, Phys. Rev. A **50**, 3827 (1994).

[32] A.D. Becke, Phys. Rev. A **38**, 3098 (1988).

[33] C. Lee, W. Yang, and R.G. Parr, Phys. Rev. B **37**, 785 (1988).

[34] J.P. Perdew, K. Burke, and Y. Wang, Phys. Rev. B (1996), (submitted).

[35] C. Froese Fischer, *The Hartree-Fock method for atoms* (Wiley, New York, 1977).

[36] S.J. Chakravorty, S.R. Gwaltney, E.R. Davidson, F.A. Parpia, and C. Froese Fischer, Phys. Rev. A **47**, 3649 (1993).